

Jets plus Missing Energy with an Autofocus

Christoph Englert,¹ Tilman Plehn,¹ Peter Schichtel,¹ and Steffen Schumann¹

¹*Institut für Theoretische Physik, Universität Heidelberg, Germany*

Jets plus missing transverse energy is one of the main search channels for new physics at the LHC. A major limitation lies in our understanding of QCD backgrounds. Using jet merging we can describe the number of jets in typical background channels in terms of a staircase scaling, including theory uncertainties. The scaling parameter depends on the particles in the final state and on cuts applied. Measuring the staircase scaling will allow us to also predict the effective mass for Standard Model backgrounds. Based on both observables we propose an analysis strategy avoiding model specific cuts which returns information about the color charge and the mass scale of the underlying new physics.

I. JETS WITH MISSING ENERGY

Missing transverse energy is a general signature for dark matter related new physics at hadron colliders [1]. It has a long history at the Tevatron and to date gives the strongest bounds on squark and gluino masses in supersymmetric extensions of the Standard Model. At the LHC the first new exclusion limits for squarks and gluinos have recently appeared, in the CMSSM toy model as well as in a more general setup [2–4]. All of these analyses are based on jets plus missing energy including a lepton veto which constitutes the most generic search strategy for strongly interacting new particles decaying into a weakly or super-weakly interacting dark matter candidate [1, 5].

While the first results are based on very inclusive cuts, following the ATLAS [6] and CMS [7] documentations we expect more specific analyses to appear soon. The reason is that in their current form the analyses can and should be optimized for specific new physics mass spectra. More specialized analyses for jets plus missing energy rely on a missing transverse momentum cut and on a certain number of staggered jet transverse momentum cuts [6, 7]. Unfortunately, they are therefore hard to adapt to modified mass spectra and by definition show a poor performance for not optimized model parameters. In addition, they are counting experiments in certain phase-space regions, which means that for any additional information on the physics behind an anomaly we have to wait for a dedicated analysis.

A major problem of searches for new physics in pure QCD plus missing energy final states is the prediction of background distributions. Aside from the improved signal-to-background ratio this is one of the reasons why applying fairly restrictive cuts on the number of jets and on their transverse momentum is a promising strategy. Such cuts relieve us from having to understand the complete p_T spectra [8] of general exclusive or inclusive n_{jets} -jet events at the LHC. Experimentally, however, we should by now be in a position to simulate these distributions using the CKKW [9, 10] or MLM [11] matching methods implemented in SHERPA [12], ALPGEN [13], or MADEVENT [14]. The different approaches have been compared in some detail, for example for W +jets production [15, 16]. What is still missing is a systematic study of theory uncertainties in multi-jet background simulations for top quark analyses and new physics searches, *i.e.* including large jet multiplicities down to intermediate jet transverse momenta, but reflecting a well defined hard scale given by the signal process. Motivated by theoretical and statistical considerations we define all observables as exclusive, specifically in the number of jets.

In this paper we establish a proper simulation of multi-jet processes and estimate these theory uncertainties, with a focus on the question what actually constitutes the theory error. This way LHC data in control regions can be used to understand very generic scaling features (*staircase scaling**) which have already been observed in data [18, 19] and which we can extend based on appropriate Monte Carlo studies. This staircase scaling we can reproduce and study using QCD Monte Carlo simulations, including different hard processes and the effects of cuts. Combining these simulations with LHC data should give us a quantitative handle on multi-jet rates in many applications.

Moreover, we can use our knowledge about the exclusive n_{jets} distributions to predict other notoriously difficult multi-jet observables. So once we understand the uncertainties on the multi-jet spectra we turn to the effective mass. In its many incarnations it either includes the leading jet or it does not and is either limited to four jets or any other number of jets [20]. Obviously, any specific definition of this mass variable increases its sensitivity to theory uncertainties. We study the most generic definition of the effective mass including *all jets* visible above

*Staircase scaling for jet rates is often referred to as Berends scaling. However, to our best knowledge it was first introduced and discussed by the authors of Ref. [17].

a transverse momentum threshold. The theory uncertainties of this observable can be closely linked to the jet-multiplicity distribution. Using the scaling properties of the exclusive jet multiplicities we can strongly reduce the theory uncertainty in the effective-mass spectrum in a consistent manner. The same should be true for other variables which we can use to extract new physics from jet dominated backgrounds.

Similar questions are currently being asked to control regions in a purely data-driven approach. However, the conversion from background regions into the signal region either by shifting the kinematic regime or by changing the hard core processes off which we radiate jets requires a good understanding for example of the effects of background rejection cuts and of background sculpting features in the definition of these observables. These effects we can reliably estimate in an appropriate Monte Carlo study and then combine for example with an over-all normalization from data.

Finally, we suggest an analysis strategy which on the one hand makes maximum use of the jet patterns and on the other hand does not require any tuning of cuts. The only ingredient of our analysis which does not involve jets is a missing transverse energy cut to reduce pure QCD backgrounds and an isolated lepton veto against W +jets backgrounds. To reduce both of them to a manageable level we require

$$\cancel{p}_T > 100 \text{ GeV} \quad \text{and a lepton veto if } p_{T,\ell} > 20 \text{ GeV}, |y_\ell| < 2.5 \quad (1)$$

as the basic and only electroweak cuts to reduce the QCD background. The exact numbers are not very dependent on the details of the model as long as the new physics sector provides a WIMP dark matter candidate. To account for fake missing energy from QCD jets we apply an additional factor of 1/500 for pure QCD and hadronic top-quark final states. This rough fake rate we estimate from Ref. [2]. It provides us with a rather conservative estimate compared e.g. to Ref. [7].

After these very generic acceptance cuts a two-dimensional correlation of the effective mass vs the exclusive jet multiplicity is the appropriate distribution to extract limits on strongly interacting new physics or in the case of an excess study the mass scale as well as the color charge of the new states. Because all our observables are defined jet-exclusively we can to a good approximation study this two-dimensional distribution using a log-likelihood shape analysis. The contributions of different regions in the $n_{\text{jets}}-m_{\text{eff}}$ space to the binned log-likelihood automatically focus on the correct phase-space region and are readily available for improved analyses as well as theoretical interpretation.

II. JET NUMBER SCALING

To separate new physics events from a QCD sample after some very basic cuts we have to understand the number of jets and their energy or p_T spectra. This will allow us to exploit two distributions: the number of jets observed (n_{jets}) and their effective mass (m_{eff}), where the definition of the latter usually requires us to define the number and hardness of the jets included in its construction. Our maximally inclusive approach means that aside from the fiducial volume of the detectors all we fix is the algorithmic jet definition to count a jet towards each of the two measurements. Throughout this paper we define jets using the anti- k_T algorithm [21] in FASTJET [22] with a resolution $R_{\text{anti-}k_T} = 0.4$ and then require

$$p_{T,j} > p_T^{\text{min}} = 50 \text{ GeV} \quad \text{and} \quad |y_j| < 4.5. \quad (2)$$

This defines which jets are counted towards n_{jets} as well as the m_{eff} distribution. Given p_T^{min} we can then evaluate the 2-dimensional n_{jets} vs m_{eff} plane in Section V using a binned log-likelihood approach.

Before we can use the n_{jets} distribution to extract new physics in the jets plus missing energy sample at the LHC we need to show that we understand this distribution in detail. Obviously, the overall normalization of this distribution is not critical. For any kind of new physics not completely ruled out by the Tevatron experiments the two jet and three jet bins are practically signal free. So the question becomes: what can we say about the shape of $d\sigma/dn_{\text{jets}}$.

For W +jets events this kind of distribution has been studied, even at the LHC [19]. We observe the *staircase scaling* [17, 23], an exponential drop in the inclusive n_{jets} rates with constant ratios $\hat{\sigma}_{n+1}/\hat{\sigma}_n$. The numerical value of this ratio is obviously strongly dependent on p_T^{min} . The original staircase scaling describes inclusive jet rates, i.e. it uses $\hat{\sigma}_n$ including all events with at least n jets fulfilling Eq.(2). In the light of recent advances in QCD and because our likelihood analysis should be based on independent bins we define the scaling in terms of exclusive jet rates, i.e. counting only events with exactly n jets fulfilling Eq.(2) towards σ_n . This preserves the normalization of the n_{jets} histogram as $\sigma_{\text{tot}} = \sum_n \sigma_n$ and makes it possible to add the bins in the computation of the log-likelihood. It is interesting to note that staircase scaling defined either way implies staircase scaling using the other definition, and

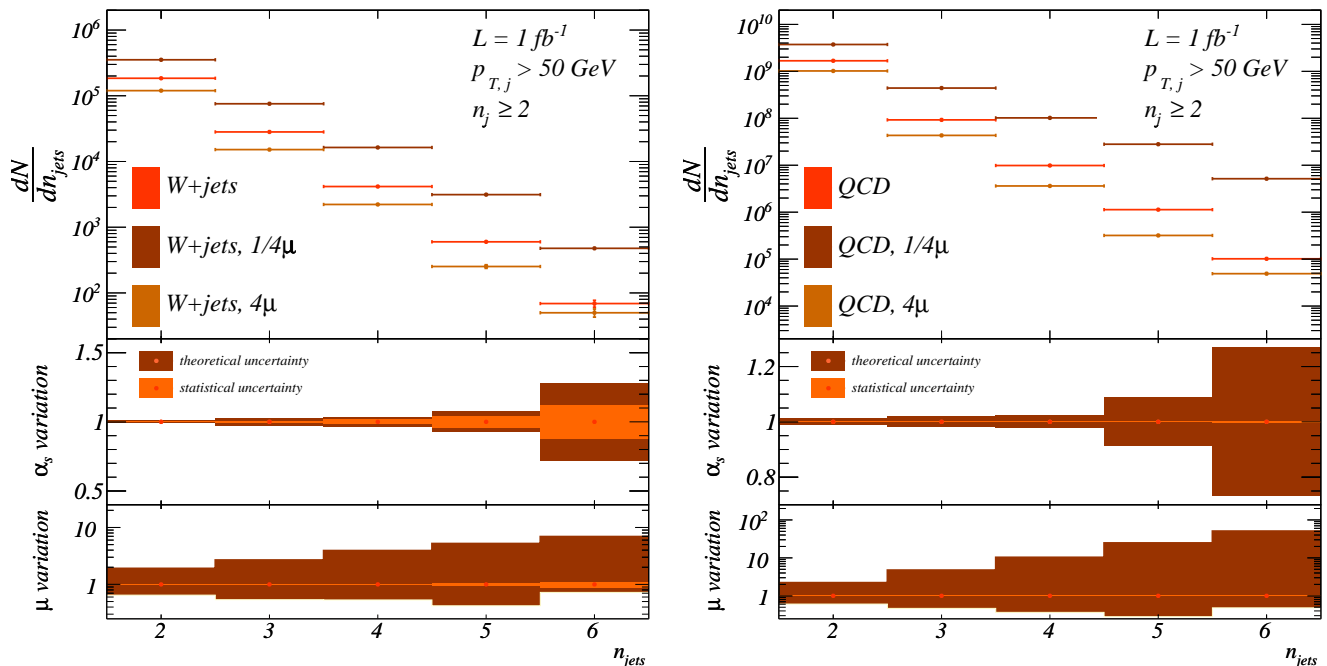


Figure 1: Exclusive $d\sigma/dn_{\text{jets}}$ distribution for W +jets (left) and QCD jets production at the LHC. Only the jet cuts given in Eq.(2) are applied, neither a p_T cut nor a lepton veto is imposed. The second panel shows the parametric uncertainty due to a consistent change of $\alpha_s(m_Z)$ between 0.114 and 0.122. The third panel shows the reach of a consistent scale factor treatment which can be experimentally determined and should not be considered a theory uncertainty.

that the jet-production ratios of the two approaches are identical. If we define the universal exclusive staircase-scaling factor as

$$R \equiv R_{(n+1)/n} = \frac{\sigma_{n+1}}{\sigma_n}, \quad (3)$$

we find for the usual inclusive scaling denoted by a hat over all parameters

$$\hat{R} \equiv \frac{\hat{\sigma}_{n+1}}{\hat{\sigma}_n} = \frac{\sigma_{n+1} \sum_{j=0}^{\infty} R^j}{\sigma_n + \sigma_{n+1} \sum_{j=0}^{\infty} R^j} = \frac{R\sigma_n}{(1-R)\sigma_n + R\sigma_n} = R. \quad (4)$$

The same relation we find when we include a finite upper limit to the number of jets in the sum over j . Note, however, that this argument only holds for a strict staircase scaling where the ratio $R_{(n+1)/n}$ does not depend on the number of jets n . For our analysis this means that we can use the staircase scaling for a statistical analysis of the $d\sigma/dn_{\text{jets}}$ distribution either in its inclusive or in its exclusive version, the latter based on independent n_{jets} bins.

In this section we will show that (1) such a scaling exists not only for W/Z +jets but also for pure QCD events and (2) we can reliably estimate the scaling factor and possible deviations from it from theory. A purely data-driven background analysis of this distribution might be possible and should be combined with our results. For example, we can one by one remove the missing energy cut and the lepton veto in Eq.(1) which gives us background dominated event samples to a reasonably large number of hard jets. Adding the background rejection cuts will then have an impact on the scaling, which we can estimate reliably. For the signal hypothesis we have to entirely rely on QCD predictions.

As a starting point we discuss the established staircase scaling in W +jets production. The behavior of Z +jets is exactly the same. For our analysis we produce CKKW-matched [10] background samples for W +jets (to 5 ME jets), Z +jets (to 5 ME jets), $t\bar{t}$ +jets (to 2 ME jets), and QCD jets (to 6 ME jets) with SHERPA-1.2.3 [12]. Higher order corrections to the inclusive scaling we expect to, if anything, improve the assumption of a constant jet ratio \hat{R} for example in W +jets production [24].

In the left panel of Figure 1 we show the exclusive n_{jets} distribution for the LHC running at 7 TeV center of mass energy. To increase our statistics to large enough values of n_{jets} we do not apply the selection cuts Eq.(1) in this first

step. We already see that we can qualitatively fit a line through the central points on a logarithmic axis for each set of input parameters.

Before we quantitatively evaluate this scaling we need to consider the uncertainties associated with our simulation. This is crucial if we want to use the n_{jets} scaling as a background estimate for new physics searches in QCD final states. There are two distinct sources of uncertainty in our simulation. First, there exists a parametric uncertainty, namely the input value of $\alpha_s(m_Z)$ or some other reference scale. To address this, we consistently evaluate the parton densities around the central NLO value $\alpha_s(m_Z) = 0.118$ inside a window $0.114 - 0.122$ [25] and keep this value for all other appearances of the strong coupling in our matrix-element plus parton-shower Monte-Carlo simulations. In Figure 1 we see that the resulting error bar on the $d\sigma/dn_{\text{jets}}$ increases with the number of jets, but stays below 30% even for the radiation of six jets. For luminosities around 1 fb^{-1} the error on α_s is roughly of the same order as the experimental statistical error. Systematic errors we do not consider, even though they will at some point dominate over the statistical errors. After any kind of realistic background rejection the combined experimental error will exceed the parametric α_s uncertainty.

The reason why we cannot use staircase scaling in W +jets to measure α_s is a second source of QCD uncertainty: aside from the parametric α_s error band, an actually free parameter in our QCD simulation is a common scaling factor μ/μ_0 in all appearances of the factorization and renormalization scales, including the starting scale of the parton shower. Identifying all scales follows the experimental extraction of the parton densities and α_s in a simultaneous fit. The interpretation of DGLAP splitting in terms of large logarithms tells us that the factorization and renormalization scales have to be identified with the transverse momentum of the radiated jets. By definition, such leading-logarithm considerations leave open the proportionality factor in the relation $\mu \propto |p_{T,j}|$. Any constant factor can be separated from the dangerous logarithm as a non-leading constant value.

Because this constant cannot be derived from first principles we vary it in the range $\mu/\mu_0 = 1/4 - 4$ and show the numerical result in Figure 1. As expected, the variation of the jet rates with this scaling parameter is huge — much larger than the experimental uncertainties we expect from the LHC and which we know from the Tevatron. In Figure 1 we can first of all check that introducing such a scaling factor does not seriously impact the observed staircase scaling. Counting such a constant towards the theory uncertainty is questionable if we can determine it experimentally. For example for SHERPA we know from Tevatron that the scaling factor should essentially be unity [26], which in the spirit of Monte-Carlo tuning means that for example in SHERPA the naive default parameter choice comes out as correctly describing the data. Of course, this does not have to be true for other simulation tools. An interesting question to ask once we have access to it at the LHC would be if this *per se* free parameter really is the same for different channels, like W/Z +jets and QCD jets.

In the right panel of Figure 1 we show the same distributions for pure QCD jet production. Again, not applying the cuts in Eq.(1) we observe staircase scaling, however, with some caveats for the two and three jet bins. This is related to the definition of the hard process. As expected, the scale factor μ/μ_0 has very large impact not on the existence of a staircase scaling but on the jet ratio R . The parametric uncertainty due to the error bar on $\alpha_s(m_Z)$ is again small once we vary the strong coupling consistently everywhere, staying below 30% for up to six jets. The parametric uncertainty for the pure QCD case and the W +jets case is clearly very similar. The scale factor variation $\mu/\mu_0 = 1/4 - 4$ gives an even larger band of possible ratios of cross sections, to be contrasted with a reduced statistical uncertainty compared to the W +jets case. Our argument that this over-all scale factor should be determined experimentally is therefore even more applicable for the QCD case. To date such an analysis does not exist, so while in the following we will use unity as the appropriate scale factor for SHERPA this needs to be verified experimentally.

Once we understand the size of theory uncertainties for the exclusive $d\sigma/dn_{\text{jets}}$ distribution we need to quantify the quality of the observed staircase scaling. Since the quantitative outcome will depend on the background rejection cuts we apply, we study the scaling without the cuts shown in Eq.(1), after the lepton veto only, and including the lepton veto as well as the missing energy cut. Starting from the individual $R_{(n+1)/n}$ values we fit a line through all relevant data points, as a function of n_{jets}

$$R(n_{\text{jets}}) = R_0 + \frac{dR}{dn_{\text{jets}}} n_{\text{jets}}, \quad (5)$$

and determine the slope to compare it to our prediction $dR/dn_{\text{jets}} = 0$.

In Table I we list the exclusive jet ratios as shown in Figure 1. For the W/Z +jets case we see that the radiation of one compared to a second jet off the Drell-Yan process $R_{2/1}$ does not show this scaling. The reason for this specific feature is the definition of the hard core process alluded to before. To generate the relatively hard jets and the large missing energy mimicking the signal events we need to at least consider $W/Z+1$ jet as the core process. In addition,

channel (cuts)	$R_{2/1}$	$R_{3/2}$	$R_{4/3}$	$R_{5/4}$	$R_{6/5}$	$R_{7/6}$	R_0	$\frac{dR}{dn_{\text{jets}}}$
	SHERPA simulation						linear fit	
$W+\text{jets}$ ($p_{T,j} > 50$ GeV)	0.1931(3)	0.1494(5)	0.157(1)	0.138(3)	0.115(8)	0.09(2)	0.150(1)	-0.001(1)
$W+\text{jets}$ (+ lepton veto)	0.2290(4)	0.1494(7)	0.164(2)	0.139(4)	0.12(1)	0.09(2)	0.149(1)	-0.002(1)
$W+\text{jets}$ (+ $\cancel{p}_T > 100$ GeV)	0.252(1)	0.224(2)	0.190(5)	0.16(1)	0.15(2)	0.09(4)	0.239(3)	-0.032(3)
$Z+\text{jets}$ ($p_{T,j} > 50$ GeV)	0.1463(2)	0.1504(6)	0.147(1)	0.138(4)	0.123(9)	0.07(2)	0.154(1)	-0.006(1)
$Z+\text{jets}$ (+ $\cancel{p}_T > 100$ GeV)	0.2251(6)	0.185(1)	0.166(3)	0.154(6)	0.14(1)	0.08(3)	0.193(2)	-0.018(2)
QCD jets ($p_{T,j} > 50$ GeV)	—	0.0552(1)	0.1074(5)	0.106(1)	0.125(5)	0.12(1)	0.105(2)	0.001(1)
$(t\bar{t})_{hh}+\text{jets}$ ($p_{T,j} > 50$ GeV)	3.69(9)	1.26(2)	0.67(1)	0.366(9)	0.24(1)	0.15(5)		
$(t\bar{t})_{\ell\ell/h}+\text{jets}$ ($p_{T,j} > 50$ GeV)	1.96(2)	0.851(7)	0.465(5)	0.260(5)	0.168(8)	0.12(2)		
$(t\bar{t})_{\ell\ell/h}+\text{jets}$ (+ lepton veto)	1.75(2)	0.765(10)	0.391(7)	0.228(8)	0.14(1)	0.12(3)		
$(t\bar{t})_{\ell\ell/h}+\text{jets}$ (+ $\cancel{p}_T > 100$ GeV)	1.60(5)	0.83(2)	0.49(2)	0.25(2)	0.15(2)	0.19(7)		

Table I: Jet ratios for all Standard Model channels, including (semi-)leptonic and hadronic top pairs for the central scale choice $\mu = \mu_0$. The quoted errors are statistical errors from the Monte Carlo simulation. The numbers correspond to the curves shown in Figures 1 and 2.

we do not take into account any separation criterion between the first jet and the gauge boson, which means we treat σ_1 different from all other σ_n . In Table I we see that we are lucky for the $Z+\text{jets}$ case, but we are not for the $W+\text{jets}$ case. The tricky definition of the hard process σ_1 as the base of additional jet radiation suggests that we start our staircase scaling analysis with $R_{3/2}$.

The statistical uncertainties which we show in Table I and which enter the fit of the slope as defined in Eq.(5) always increase towards larger jet multiplicity. This is an effect of the way we simulate these events which completely corresponds to an experimental analysis. If we generate (or measure) all n_{jets} bins in parallel the first bin will always have by far the smallest error. Therefore, it determines the constant scaling factor R_0 in our fit as well as in a measurement. For larger values of n_{jets} we become statistics dominated, which means that Monte Carlo simulations can extend the reach of actual measurements at any given point in time towards larger jet multiplicities. This is the phase space region in which we need to provide new physics searches at the LHC with accurate background estimates.

Some of the rows listed in Table I we also depict in Figure 2. For electroweak gauge boson production we see that without any cuts W and Z production show the same scaling parameter R_0 as well as a small negative slope. Within errors the staircase scaling holds to six and possibly seven jets, even though we see a slight slope developing towards larger numbers of jets. This is a phase space effect which is expected once we start probing gluon parton densities and their sharp drop towards larger parton momentum fractions and which is well modeled by our computation.

Adding the lepton veto does not change the staircase scaling at all. This means that forcing the W boson to

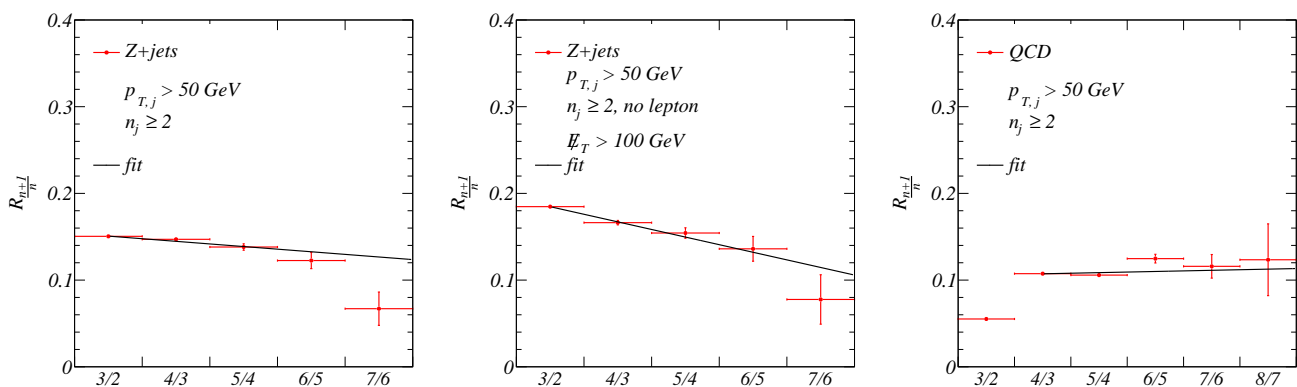


Figure 2: Jet ratios for $Z+\text{jets}$ production (without and with the $\cancel{p}_T > 100$ GeV cut) and QCD jets production, corresponding to the numbers listed in Table I. The error bars indicate the remaining Monte Carlo uncertainty in our simulation.

decay into one fairly soft lepton and a harder neutrino does not affect the behavior of the recoiling jets. Adding a significant p_T cut, on the other hand, has a measurable effect on the jet ratios as well as on the slope. For experimental applications of this scaling, however, it is important to note that the phase space effects for large n_{jets} as well as the effect of kinematic cuts are completely described by our simulation.

For pure QCD events we find a remarkable agreement with the staircase scaling hypothesis, which seems to be supported by recent LHC analyses [27]. The definition of the hard core process is somewhat problematic since there exists no inherent hard scale in the $2 \rightarrow 2$ process and the infrared behavior of s -channel and t -channel diagrams is very different. Therefore, we define σ_3 as the starting point of our analysis and $R_{4/3}$ as the first relevant cross section ratio. Table I and Figure 2 show that the ratios $R_{(n+1)/n}$ are essentially constant to eight jets. The slope within statistical uncertainties is, in contrast to W/Z production, fully compatible with zero. The central R_0 values for W/Z +jets and QCD jets production are slightly different, which is expected by the different core processes and by the different background rejection cuts.

III. DECAY JETS VS JET RADIATION

In contrast to the QCD and gauge-boson background n_{jets} distributions from heavy particles decaying to jets include two sources of jets: first, there are decay jets, which dependent on the spectrum might or might not be hard enough to stick out. Second, there is QCD jet radiation, which for heavy states will generically be relatively hard and dominated by collinear splitting in the initial state [28, 29], leading to a non-zero maximum value of the number of expected initial-state radiation jets [1, 30]. Due to the hard scale of new-physics processes on the one hand and because we need to simulate supersymmetric decays inclusively we best generate the new-physics events with HERWIG++-v2.4.2 [31] and normalize the cross sections with PROSPINO2.1 [32]. All supersymmetric mass spectra we generate with SOFTSUSY [33] using the SLHA output format [34] and use SDECAY [35] to calculate the leading-order branching ratios. We check the jet-radiation results from the HERWIG++ shower with MLM merging implemented in MADEVENT [29], using PYTHIA [36] for parton showering and hadronization. As expected, the two simulations agree well within their uncertainties.

The question for heavy-particle production is how universal its n_{jets} distributions are when we consider Standard Model as well as new-physics particles with different masses and color charges, like top quarks, squarks and gluinos. In Figure 3 we first show the n_{jets} distributions for (semi-)leptonic and hadronic top-pair production. We see how all unsubtracted distributions show maxima away from $n_{\text{jets}} = 0$, driven by the presence of decay jets plus relatively hard jet radiation. In addition, they do not show a staircase scaling at large jet multiplicities. Because the particles produced in the hard process have non-negligible masses even compared to the hadronic center-of-mass energy the phase-space suppression for example due to rapidly dropping gluon densities kicks in immediately and bends the otherwise exponential fall-off.

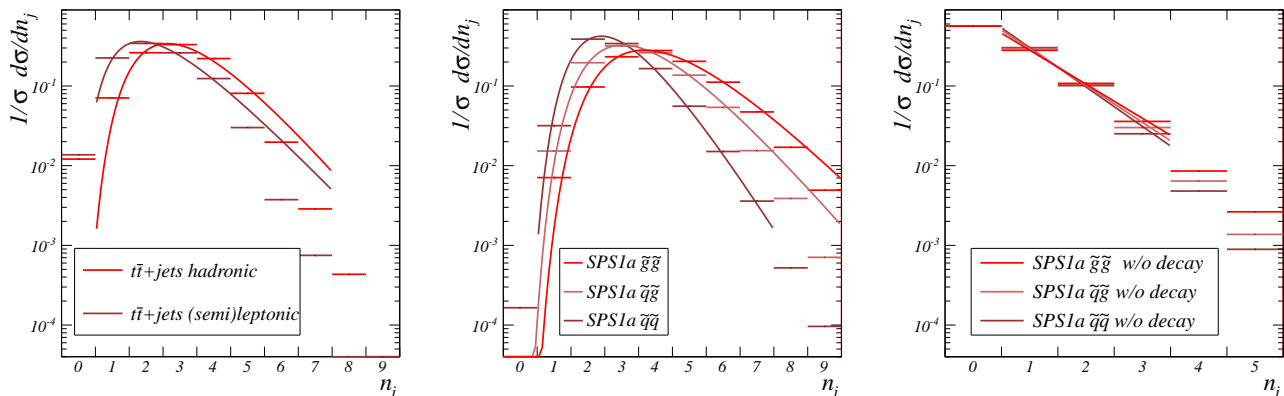


Figure 3: Normalized exclusive $d\sigma/dn_{\text{jets}}$ distributions for top pairs (left) and supersymmetric particle production. For the latter we show all decay jets plus QCD jet radiation (center) as well as QCD jet radiation only (right). Jets are counted once they fulfill Eq.(2).

	$(tt)_{hh}$	$(tt)_{\ell\ell/h}$	$\tilde{q}\tilde{q}$	$\tilde{q}\tilde{g}$	$\tilde{g}\tilde{g}$	SUSY	$\tilde{q}\tilde{q}$	$\tilde{q}\tilde{g}$	$\tilde{g}\tilde{g}$
	full		full				jet radiation		
a_0	3.13	2.34	2.89	3.53	4.16	3.15	n.a.	n.a.	n.a.
a_1	5.41	3.73	5.28	6.16	7.15	5.48	0.45	0.36	0.21
b	1.25	1.07	1.71	1.25	1.09	1.27	1.14	1.07	0.98

Table II: Parameters defined in Eq.(6) and extracted from the unsubtracted distributions shown in Figure 3. The parameter a_0 corresponds to the position of the maximum while b captures the approximate scaling at larger n_{jets} . The combined supersymmetric result is based on the appropriately weighted event samples for squarks and gluinos.

In the Standard Model we can fit the (semi-)leptonic and purely hadronic top-pair distributions for all jets fulfilling Eq.(2) to the function

$$\frac{d \log \sigma(n_{\text{jets}})}{dn_{\text{jets}}} = -b \frac{n_{\text{jets}}^2 - a_1 n_{\text{jets}} + a_0^2}{n_{\text{jets}}}. \quad (6)$$

The two relevant fit parameters for the normalized distributions shown in Figure 3 correspond to the maximum at $n_{\text{jets}} = a_0$, and the (staircase) scaling parameter for QCD jet radiation at large n_{jets} given by $R = \exp(-b)$. Because we do not include higher suppression terms towards large n_{jets} we stop the fit at the endpoints of the curves shown in Figure 3.

In Table II we list the best fit values for these parameters for both top decays. We immediately see more quantitatively than in Figure 3 that for example hadronically decaying top pairs on average include not even one more jet than the (semi-)leptonic sample. Typically only one of two jets from the W decay is accounted for because of the cutoff at $p_T^{\text{min}} = 50$ GeV. Comparing this value to the W mass it is likely that one of the two W decay jets gets boosted above p_T^{min} , but the other one stays below. In contrast, the Jacobian peak of the b -quark energy from the top decay lies above p_T^{min} . Going back to Table II this means that for top pairs the most likely number of radiated jets is zero, closely followed by one jet emission [30].

For squarks and gluinos the features we see in top-pair production become more pronounced and the jet multiplicity reflects the color charge of the produced particles. As a reference point in supersymmetric parameter space we consider reasonably low mass gluinos and squarks in the SPS1a benchmark scenario [37], with $m_{\tilde{g}} = 608$ GeV and typical light-flavor squarks around $m_{\tilde{q}} \sim 558$ GeV. The new LHC exclusion limits are right at the edge of excluding this standard parameter choice[†]. Because the gluino cannot decay to a gluon it requires two quarks to get rid of its color charge. Squark pairs, including squark-antisquark production, predict two hard decay jets plus some QCD radiation and sub-leading decay jets. In Table II we see that for this production channel the maximum of a continuous n_{jets} distribution indeed resides almost at $n_{\text{jets}} = 3$. For associated squark-gluino and gluino-pair production the number of jets increases by almost one, corresponding to the second gluino-decay jet which not in all cases is hard enough to appear after requiring $p_T^{\text{min}} = 50$ GeV. The jet multiplicity of the entire supersymmetric sample is close to the average for squark pair production and squark-gluino production which reflects the hierarchy in cross sections of the three processes [32].

Breaking down the supersymmetric signal into individual production processes we can examine the distinct radiation patterns. Gluino pairs radiate significantly more than associated production or squark pairs, which is reflected in the right columns of Table II: $b(\tilde{g}\tilde{g}) < b(\tilde{q}\tilde{g}) < b(\tilde{q}\tilde{q})$. The scaling parameter $R = \exp(-b)$ is consistently larger than for the background samples in Table I. For example for the jet radiation off squark pair production we find $R \approx 0.32$. Moreover, in Figure 3 we see that the jet rates for QCD radiation drop off even faster for large multiplicities. This means that there definitely does not exist any staircase scaling behavior for heavy particle pair production above a threshold of 1 TeV at the LHC with a hadronic center-of-mass energy of 7 TeV. This phase space argument should not be mixed with the fact that the hard scale of such processes and with it the logarithmic enhancement for collinear radiation is large, *i.e.* the validity of the collinear approximation extends to larger values of $p_{T,j}$.

Finally, in Figure 4 we show the n_{jets} distribution for the supersymmetric signal assuming the SPS1a parameter point and the various Standard Model backgrounds. We apply the background rejection cuts specified in Eqs.(1) and

[†]Due to the presentation of the LHC results in the m_0 vs $m_{1/2}$ plane it is also not possible to precisely read off the actual limits in terms of physics mass parameters. Moreover, since squark and gluino masses are both mostly driven by $m_{1/2}$, there does not exist a mapping of the m_0 - $m_{1/2}$ plane into the squark-gluino mass plane. Models with significantly heavier gluinos than quarks are excluded in CMSSM searches.

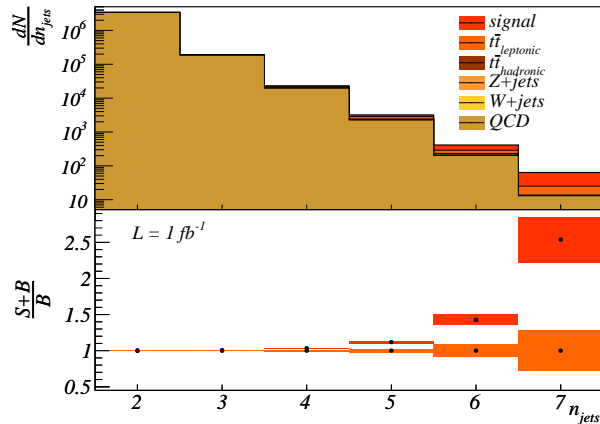


Figure 4: Exclusive n_{jets} distribution for all considered Standard-Model backgrounds and the SPS1a signal for supersymmetry. We present the results for an LHC center-of-mass energy of 7 TeV with an integrated luminosity of 1 fb^{-1} and after the cuts specified in Eqs. (1) and (2).

(2). The variation in shape when including the signal events is statistically significant and appears as an excess of high jet-multiplicity events for $n_{\text{jets}} > 5$. The associated statistical significance we compute in Section V.

IV. EFFECTIVE MASS

Before we turn to exploit the number of jets to extract a new physics signal at the LHC an obvious question is if we can make use of our understanding of the n_{jets} distribution looking at other observables in multi-jet final states. More specifically, we will use the measured scale parameter μ/μ_0 shown in Figure 1 to reliably predict observables, which, based on traditional QCD simulations, show an overwhelming theory uncertainty. A classic observable in this respect is the effective mass [20], which for exclusive jet multiplicities we define as

$$m_{\text{eff}} = \not{p}_T + \sum_{\text{all jets}} p_{T,j} , \quad (7)$$

including all jets fulfilling Eq.(2). This definition is neither optimized to take into account a correlation between hard jets and the missing-energy vector nor to remove hard initial-state radiation. Instead, Eq.(7) makes a minimal set of assumptions to avoid sculpting the background distribution.

Just like the n_{jets} distribution m_{eff} in the Standard Model cannot be reliably predicted by parton-shower Monte Carlos. Jets entering the sum in Eq.(7) we have to understand over their entire transverse-momentum spectrum. CKKW [9, 10] or MLM [11] matching is therefore the most adequate approach for simulating m_{eff} .

Exactly following the treatment of the n_{jets} distribution in Section II we estimate two sources of theory uncertainties, the parametric error from varying the strong coupling and the scale-variation systematics. To not be limited by statistics of our background samples we for now discard the missing energy cut and the lepton veto and instead study the fully inclusive processes. In Figure 5 we present the m_{eff} distribution for W +jets and the QCD jets production with $n_{\text{jets}} \geq 2$. The same way as in Figure 1 we show the relative impact of the two sources of uncertainty in the lower panels. The parametric error from $\alpha_s(m_Z)$ ranges well below 20% even towards large values of m_{eff} . For the electroweak process this is of similar size to the expected statistical error for an integrated luminosity of 1 fb^{-1} . As expected, towards large m_{eff} the error band increases, but not dramatically.

In contrast, the scale-factor variation $\mu/\mu_0 = 1/4 - 4$ has a huge effect on the m_{eff} simulation, essentially rendering it unpredictable. For values above $m_{\text{eff}} = 500 \text{ GeV}$ the error bands become large enough to make it impossible to extract new physics from this observable, were we to consider the scale variation a proper theory error. However, measurements of multi-jet rates and other jet observables at Tevatron and LHC indicate that for the case of SHERPA this scaling factor is approximately one [26]. Measuring the staircase-scaling factors even more precisely with the 2011 LHC data will further constrain the scale ambiguities underlying our QCD simulations – allowing us to make reliable predictions for e.g. the m_{eff} observable.

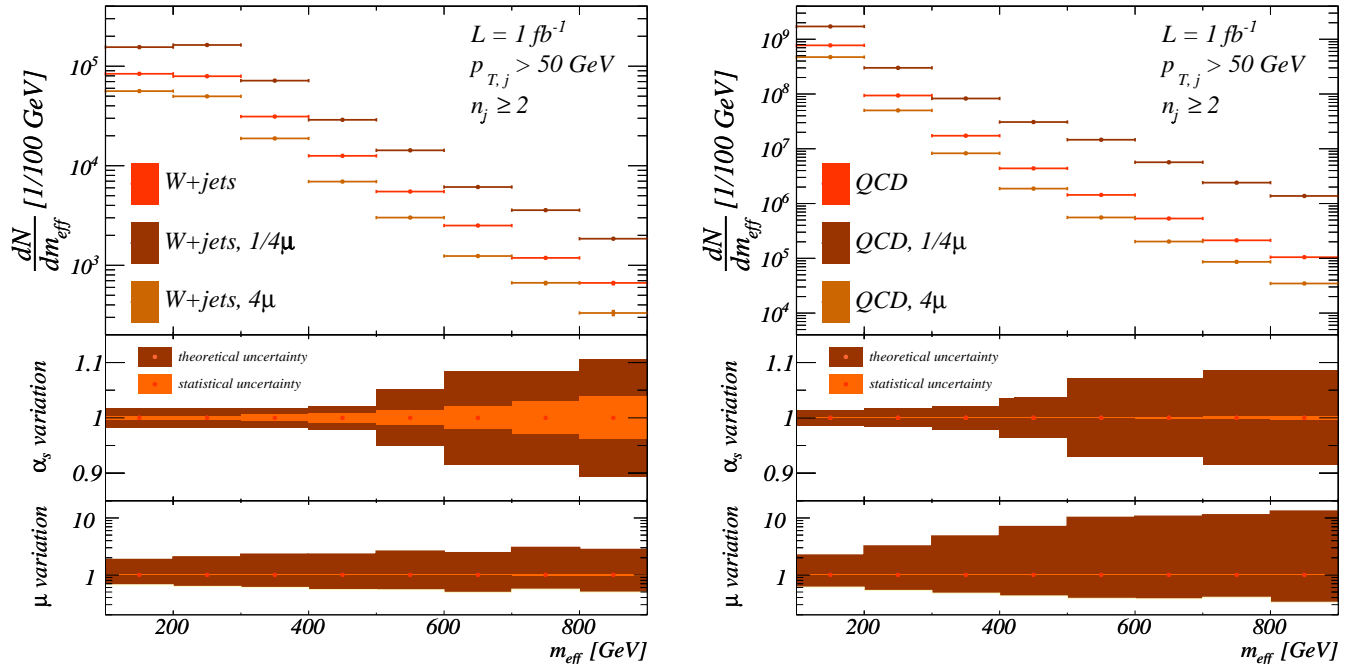


Figure 5: Effective mass distribution for W +jets and QCD jets production. Only the jet cuts given in Eq.(2) are applied. The second panels show the parametric uncertainty due to a consistent change of $\alpha_s(m_Z)$ between 0.114 and 0.122. The third panels show a consistent scale factor variation which can be experimentally constrained and should not be considered a theory uncertainty.

To see the impact of m_{eff} in searches for supersymmetry we show the m_{eff} distribution for exclusive 2-jet and 3-jet events in Figure 6. It includes Standard-Model backgrounds as well as the supersymmetric signal. All jet-selection and background-rejection cuts specified in Eqs.(1) and (2) are applied. As mentioned before, QCD jets are the by far dominant channel. Only for $m_{\text{eff}} > 800$ GeV the signal starts overcoming the backgrounds. The statistical uncertainty for 1 fb^{-1} we indicate by the shaded regions in the lower panels. It is worth noticing that the signal+background sample when compared to the pure background sample exhibits a maximum at around $m_{\text{eff}} \sim 1.1$ TeV. This scale corresponds to the squark and gluino masses which for pair production add to 1100 to 1200 GeV. This means that the m_{eff} distribution for exclusive jet multiplicities can serve as background rejection as well as a measure for the mass scale of the new heavy colored states.

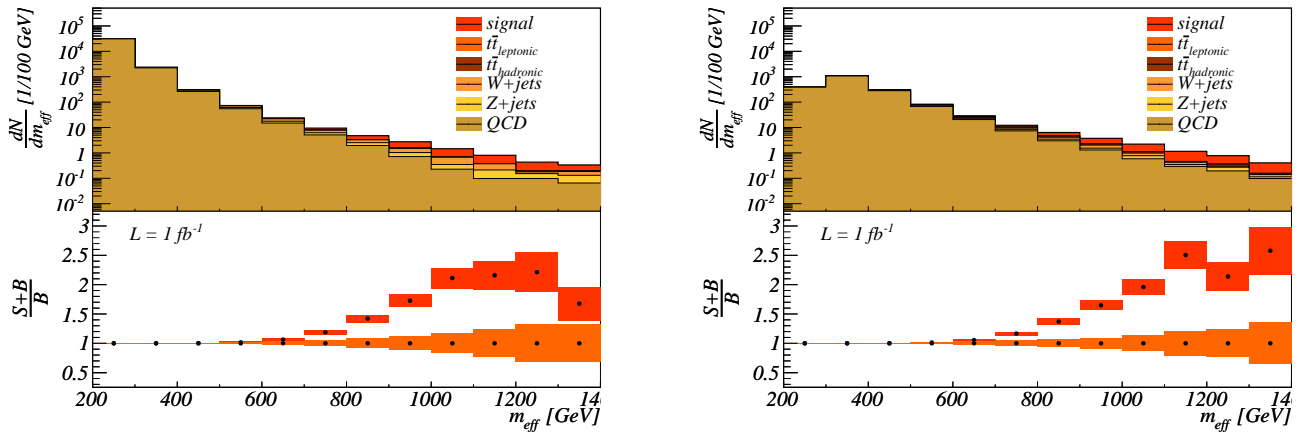


Figure 6: Effective mass distribution for exclusive 2-jet and 3-jet events for Standard-Model backgrounds and the supersymmetric signal using the SPS1a parameter point. We assume a center-of-mass energy of 7 TeV with an integrated luminosity of 1 fb^{-1} and apply all cuts in Eqs.(1) and (2).

	signal significance for 35 pb ⁻¹
inclusive	0.2 σ
n_{jets} (1D)	1.6 σ
m_{eff} (1D)	3.3 σ
$(n_{\text{jets}}, m_{\text{eff}})$ (2D)	4.6 σ

Table III: Confidence levels for the signal plus background sample ruling out the background-only hypothesis based on one and two dimensional log-likelihood distributions. The supersymmetric mass spectrum is given by SPS1a.

V. AUTOFOCUSING

Following our results in the previous sections we should be able to use the shapes of the n_{jets} and m_{eff} distributions to extract a supersymmetric signal from the now quantitatively understood Standard Model backgrounds. Given that the two distributions are affected independently by the color structure of the new physics sector and by its mass scale(s) we will assess the power of the two-dimensional n_{jets} vs m_{eff} correlations in extracting a discovery or an exclusion. Such a two-dimensional shape analysis is the natural second step after the first completely inclusive searches based on counting events. According to Sections II-IV systematic experimental uncertainties will start dominating for luminosities around $\mathcal{O}(1 \text{ fb}^{-1})$. Since those are subject to continuous refinement during data taking and need to be addressed within a full detector simulation study we limit ourselves to statistical uncertainties for a given luminosity. While this means that we will not obtain reliable estimates for the discovery reach, we will see that it allows us to discuss the main benefits and limits of the proposed analysis.

As supersymmetric reference models we choose the benchmark point SPS1a, two variations of it, and SPS4. Again, we only apply the cuts given in Eqs.(1) and (2) and use the exclusive definition of n_{jets} and m_{eff} . For the m_{eff} distribution we choose a binning of 100 GeV, which approximately reflects the experimental resolution towards large m_{eff} .

For given background and signal+background hypotheses we use a binned log-likelihood ratio to compute statistical significances assuming statistically uncorrelated bins

$$\log Q = \sum_{\text{bins}} \left[n_i \log \left(1 + \frac{s_i}{b_i} \right) - s_i \right]. \quad (8)$$

It includes the luminosity via the signal and background event numbers s_i and b_i in each bin. While it avoids the limitations of S/\sqrt{B} in regions requiring Poisson statistics it approaches a Gaussian limit for each individual channel when the bin content becomes large. Some features of this well established approach we summarize in Appendix A. Applying a “simple hypothesis test” tells us how likely it is that the background-only hypothesis fakes the predicted signal+background distributions as a statistical fluctuation, *i.e.* we define the p -value as the SPS1a likelihood ratio’s median. The likelihood ratio given in Eq.(8) we compute for the exclusive n_{jets} , m_{eff} , and two-dimensional $(n_{\text{jets}}, m_{\text{eff}})$ distributions. In this two-dimensional plane the definition of m_{eff} , following Eq.(7), only includes exactly n_{jets} jets. With this completely exclusive definition of n_{jets} and m_{eff} we ensure that the sum over all bins in the $(n_{\text{jets}}, m_{\text{eff}})$ reproduces the total cross section.

Considering this correlation is similar in spirit to the (\cancel{p}_T, H_T) analysis proposed in Ref. [38]. However, first we focus on the n_{jets} and m_{eff} distributions because in Sections II-IV we have shown that we can quantitatively understand the staircase scaling behavior of the Standard Model backgrounds and translate its precision into other variables. In addition, as we will see in this section these two variables play a special role, as they not only distinguish signals from backgrounds, but also contain information on the structure of the underlying new-physics model. As mentioned above, for the sake of a proof of concept we ignore all uncertainties except for statistical experimental errors, to avoid correlations in the definition of the log-likelihood.

We can expect from Figures 4 and 6 that the rate in each individual n_{jets} bin is dominated by Standard-Model processes at low m_{eff} . Most likely, this region will be the control region to normalize the QCD and W/Z +jets backgrounds. With the exception of hadronically decaying top pairs all Standard-Model channels will then show a simple decrease in both directions of the two-dimensional $(n_{\text{jets}}, m_{\text{eff}})$ plane which we can predict following the arguments in Sections II-IV. The signal contribution will become visible only once m_{eff} reaches the mass range of the particles produced.

In Table III we compare the statistical significances for the supersymmetric SPS1a parameter point at 7 TeV center-of-mass energy for the various analysis strategies: first, we show the results based on the total production rates after the inclusive cuts of Eqs.(1) and (2). As expected, including the signal events leaves us completely consistent with the background-only hypothesis. Next, the likelihood ratio computed from the n_{jets} distribution gives rise to sizable deviations from the background for integrated luminosities as small as 35 pb^{-1} . The one-dimensional m_{eff} distribution turns out to be an even better discriminator. It gives us more than twice the n_{jets} significance, namely 3.3σ for $\mathcal{L} = 35 \text{ pb}^{-1}$. The highest significant discriminative power we obtain for the two-dimensional binned $(n_{\text{jets}}, m_{\text{eff}})$ case. This is a direct consequence of the additive binned log-likelihood given in Eq.(8).

Beyond the relevance of the $(n_{\text{jets}}, m_{\text{eff}})$ distributions to extract new particles from backgrounds, we can utilize it to study signal properties. Above, we argue that new physics contributions to n_{jets} will only appear once m_{eff} reaches the mass scale of the sum of both heavy particles produced. However, this only happens if the exclusive n_{jets} value allows us to include the decay jets contributing to m_{eff} . Hence, the new physics contributions to the two observables will show a correlation based on the mass and decay channels of the new particles produced. The decay channels can typically be linked to the color charge of the new particles if we assume that the missing energy particle cannot carry color charge. Color triplets will tend to decay to one hard quark jet while color octets with their diagonal coupling to gluons will radiate two quark jets. This means breaking down the binned log-likelihood ratio over the fully exclusive $(n_{\text{jets}}, m_{\text{eff}})$ plane and keeping track of the individual contribution of each bin will automatically focus our search on the appropriate properties of the particles we are looking for.

This statement is not limited to supersymmetry, the SPS1a parameter point or any other assumption about the signal. It can be applied to general physics beyond the Standard Model with strongly interacting new particles and a stable dark matter candidate. In Figure 7 we show the contributions of the individual bins to the summed log-likelihood ratio for all signal events combined and split into three production processes. The maximum significance automatically reflects SPS1a's decay paradigm $\tilde{q}\tilde{q}^{(*)} \rightarrow 2 \text{ jets}$ and $\tilde{q}^{(*)}\tilde{g} \rightarrow 3 \text{ jets}$, and $\tilde{g}\tilde{g} \rightarrow 4 \text{ jets}$, know already from Figure 3. The first two channels we can study using an integrated luminosity of 1 fb^{-1} . Squark pair production is dominant because at the LHC it includes a quark-quark initial state. Associated production, which often is the dominant channel at the LHC, has a comparable statistical yield and features a slightly higher m_{eff} range. Both channels combined define the diagonal correlation we see for the combined signal events.

Gluino pair production has the smallest production rate and therefore becomes subleading in the combined supersymmetry sample. However, for this channel we can best follow the imprint of higher jet multiplicities. Due to its large mass and its color charge gluino pairs produce significantly more jet radiation which we can resolve for a sufficiently low p_T^{min} threshold. For $p_T^{\text{min}} = 50 \text{ GeV}$ we might just capture the first decay jet from the gluino cascade, reflecting the mass hierarchy $m_{\tilde{g}} - m_{\tilde{q}} \sim 60 \text{ GeV}$. The peak in the log-likelihood plane around $n_{\text{jets}} = 4$ results from the maximum in the $\tilde{g}\tilde{g}$ production cross section. For $n_{\text{jets}} = 5$ the background is still large compared to the signal, but dropping at an exponential rate it gets surpassed for $n_{\text{jets}} = 6$, explaining the structure we observe in Figure 7.

Finally, we can study how changes to the new physics spectrum are reflected in the significances computed from the binned log-likelihood $Q(n_{\text{jets}}, m_{\text{eff}})$. We investigate three different supersymmetric mass spectra : first, we increase only the gluino mass by 150 GeV with respect to SPS1a ($\sigma_{\text{SUSY}}^{\text{NLO}} = 2.69 \text{ pb}$ according to PROSPINO2.1 [32]); second, we increase all colored-sparticle masses by 100 GeV with respect to SPS1a ($\sigma_{\text{SUSY}}^{\text{NLO}} = 1.63 \text{ pb}$); third, we consider the SPS4 benchmark [37] with an inverted mass hierarchy $m_{\tilde{q}} \sim 750 \text{ GeV} > m_{\tilde{g}} \sim 730 \text{ GeV}$ ($\sigma_{\text{SUSY}}^{\text{NLO}} = 0.83 \text{ pb}$). All of these cross sections are significantly smaller than for SPS1a with its $\sigma_{\text{SUSY}}^{\text{NLO}} = 4.68 \text{ pb}$, which means we increase our nominal luminosity to $\mathcal{L} = 5 \text{ fb}^{-1}$.

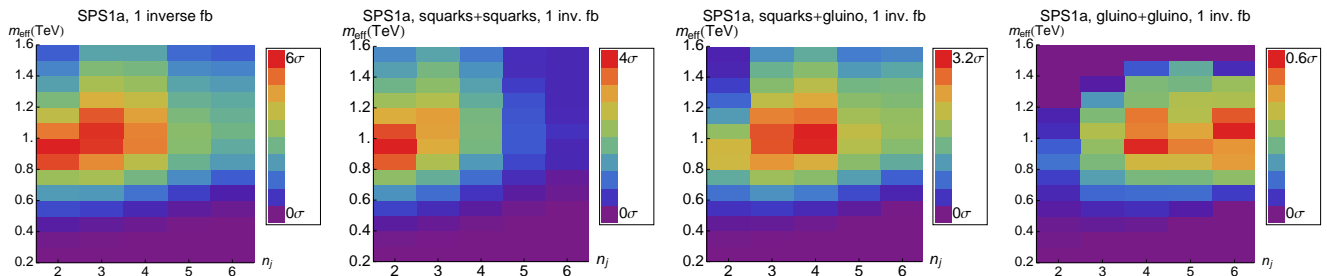


Figure 7: Log-likelihood contributions over the $(n_{\text{jets}}, m_{\text{eff}})$ plane for the supersymmetric signal using the SPS1a spectrum. The color code is normalized to different maximum significances.

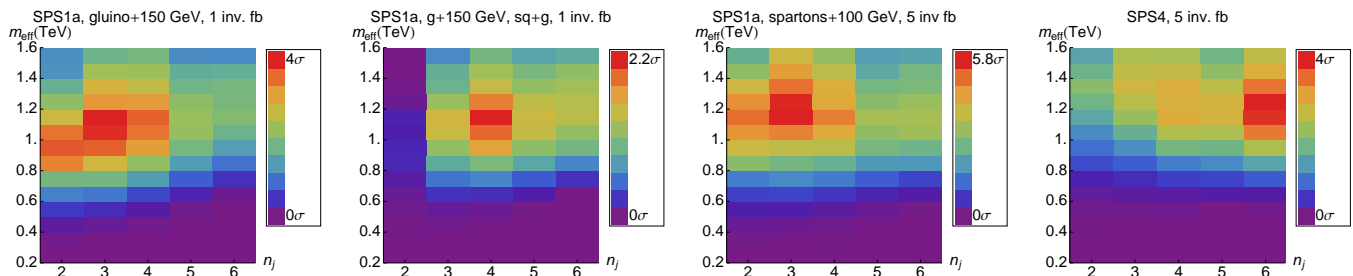


Figure 8: Log-likelihood distributions over the $(n_{\text{jets}}, m_{\text{eff}})$ plane for the different supersymmetric spectra. Due to the smaller signal rates we present results for an integrated luminosity of 5 fb^{-1} .

In Figure 8 we clearly see the effect of the increased gluino mass. The m_{eff} peak for associated squark-gluino production moves to larger values, as does the n_{jets} maximum. However, because the balance between squark pair production and associated squark-gluino production shifts into the direction of the squark pairs, this effect is not quite as pronounced. The second scenario with increased squark and gluino masses leads to a pronounced maximum at larger m_{eff} . Due to the smaller signal cross section the sensitivity in particular in the $n_{\text{jets}} = 2$ bins gets considerably diminished, appearing as a shift towards higher n_{jets} values. For the all-hadronic search in the SPS4 parameter point longer decay chains for gluinos through bottom squarks appear in the high n_{jets} bins only.

The SPS4 case illustrates that $n_{\text{jets}} = 6$ does not have to be the maximum jet multiplicity we need to consider. Once we rely on a combination of data and Monte Carlo methods to describe the n_{jets} staircase scaling for background processes we can extend our analyses to very large jet multiplicities. On the other hand, Figure 7 also clearly indicates that for example in the SPS1a parameter point the optimal signal extraction strategy by no means requires us to go to very large jet multiplicities. For the SPS1a parameter point the two-jet bins are leading contributions to the total significance.

VI. OUTLOOK

Multi-jet events with and without a weak gauge boson are the dominant backgrounds to inclusive searches for example for supersymmetry. Simulating them with traditional parton shower Monte Carlos does not lead to reliable results. This changes when we make use of jet merging to predict the shapes of multi-jet backgrounds.

One of the most challenging distributions to describe theoretically is the inclusive or exclusive number of jets per event. From data we know that the inclusive W/Z +jets distributions without rigid cuts follow a *staircase scaling* with constant jet ratios $R = \hat{\sigma}_{n+1}/\hat{\sigma}_n$. We have shown that staircase scaling in the inclusive jet rates is equivalent to the same scaling in exclusive rates. Nowadays, the exclusive scaling we can compare to the predictions of jet merging Monte Carlos, like SHERPA. Moreover, we have seen that QCD jet production shows an even more pronounced scaling than W/Z +jets production to jet multiplicities of $n_{\text{jets}} = 8$.

We studied the validity of the staircase scaling behavior, the theory uncertainties in the n_{jets} distributions, its link to other multi-jet observables, and the application of jet-exclusive observables to new physics searches and found:

1. While we cannot derive the staircase scaling of the n_{jets} distribution from first principles we can reproduce it using the appropriate Monte Carlo tools. This includes the scaling feature itself, a careful error analysis, and the scaling violation effects towards large values of n_{jets} due to phase space restrictions.
2. The theory uncertainty on the staircase scaling consists of tunable parameters like scale factors in the factorization and renormalization scales and on parametric errors like the dependence on α_s . The latter are small. The scale factor hugely overestimates the error and should be thought of as a tuning parameter for the different jet merging implementations. For SHERPA it comes out close to unity.
3. The scaling parameter $R = \sigma_{n+1}/\sigma_n$ depends on the hard process and on kinematic cuts. Both effects we can reliably predict using Monte Carlos, as we have shown for the W/Z +jets and pure jets cases. The γ +jets case we postpone to a later study with more specific details for the LHC experiments [39].

4. These simulations of the staircase scaling in multi-jet processes can be easily combined with data driven techniques, giving us the over-all normalization and a cross check for the first n_{jets} bins. Statistically limited regions of phase space will become accessible via simulations, including a reliable error estimate.
5. Understanding staircase scaling of multi-jet processes allows us to predict other multi-jet variables, like the effective mass m_{eff} . Again, this includes a proper treatment of theory uncertainties. In addition, the completely inclusive definition of m_{eff} removes dangerous artifacts due to the usual truncations.
6. Based on for example the n_{jets} vs m_{eff} correlation for a fixed p_T^{min} we can define a likelihood-based analysis avoiding model or spectrum specific background rejection cuts. Such shape analyses in multi-jet search channels are the natural extension of the early inclusive ATLAS and CMS searches.

Of course this simple first approximation to the exclusive zero-lepton search for jets plus missing energy is not the only application of such methods. Searches including leptons, b tags, or hard photons will benefit from the same treatment, as long as they include non-negligible numbers of jets. The same is true for hadronically decaying top quarks in the Standard Model.

Acknowledgments

We would like to thank Elmar Bittner and Andreas Nussbaumer for computing support. All simulations underlying this study have been performed on bwGRiD (<http://www.bw-grid.de>), member of the German D-Grid initiative, funded by the Ministry for Education and Research (Bundesministerium für Bildung und Forschung) and the Ministry for Science, Research and Arts Baden-Württemberg (Ministerium für Wissenschaft, Forschung und Kunst Baden-Württemberg).

Appendix A: Hypothesis test

In this section we briefly review the binned log-likelihood ratio hypothesis tests which we apply in Section V. It discriminates between two specific hypotheses and has been used for the combined LEP-Higgs limits [40], Tevatron analyses [41], and in various contexts of LHC Higgs phenomenology [42]. According to the Neyman–Pearson lemma [43] the likelihood ratio is the most powerful test statistic (e.g. signal+background vs background-only). We compute the (binned) log-likelihood ratio

$$Q = -2 \log \frac{L(\text{data} | \mathcal{S} + \mathcal{B})}{L(\text{data} | \mathcal{B})} = 2 \left[s - n \log \left(1 + \frac{s}{b} \right) \right] \stackrel{\text{binned}}{=} 2 \sum_{i \in \text{bins}} \left[s_i - n_i \log \left(1 + \frac{s_i}{b_i} \right) \right], \quad (\text{A1})$$

where s and b denote the signal \mathcal{S} and background \mathcal{B} event numbers for a given luminosity, split into the bins i . The probabilities to observe n events given the expected numbers s and b in Eq.(A1) are determined by Poisson

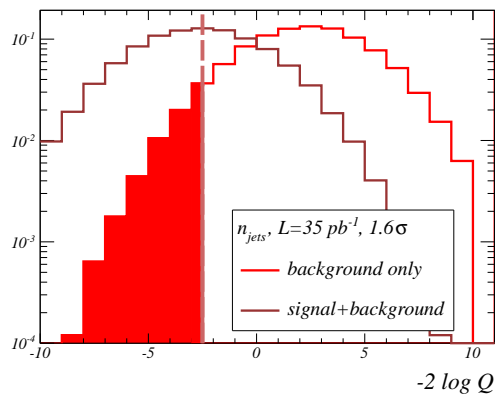


Figure 9: Log-likelihood ratio distributions based on the n_{jets} discriminator for a luminosity of 35 pb^{-1} . The confidence level is computed by evaluating the overlap of the background-only distribution with the signal+background maximum.

distributions

$$L(\text{data} | \mathcal{S} + \mathcal{B}) = \frac{(b+s)^n e^{-(s+b)}}{n!} \qquad L(\text{data} | \mathcal{B}) = \frac{b^n e^{-b}}{n!} . \quad (\text{A2})$$

The sum in Eq.(A1) extends over all contributing channels. The likelihood distributions we generate as pseudo-data around each hypothesis' central value, which means that in principle we can include any kind of correlation. In this work we limit ourselves to statistically independent bins i of the n_{jets} and m_{eff} distributions. The set of entries in each bin $\{n_i\}$ we simulate numerically and histogram them as a function of \mathcal{Q} , following the Neyman-Pearson lemma. To simulate the log-likelihood distributions we need to specify which hypothesis the bin entries $\{n_i\}$ should follow, *i.e.* we can compute $\mathcal{Q}_{\mathcal{S}+\mathcal{B}}$ or $\mathcal{Q}_{\mathcal{B}}$. In Figure 9 we show both \mathcal{Q} distributions for the binned one-dimensional n_{jets} distribution studied in our paper.

In our analysis we are interested in the probability that the background alone fakes the expected signal+background distributions. This confidence level is given by the integral of the background distribution $\mathcal{Q}_{\mathcal{B}}$ over the signal+background range, indicated by the red-shaded region in Figure 9. This signal+background range is defined as all likelihood values above the median of the likelihood distribution assuming the signal+background hypothesis

$$\text{CL}_{\mathcal{B}} = \int_{-\infty}^{(\mathcal{Q}_{\mathcal{S}+\mathcal{B}})} \mathcal{Q} \mathcal{Q}_{\mathcal{B}} = \text{erfc} \left(\frac{Z}{\sqrt{2}} \right) , \quad (\text{A3})$$

where for illustration purposes we convert the confidence levels into the Gaussian number of standard deviations Z via the inverse error function.

-
- [1] D. E. Morrissey, T. Plehn and T. M. P. Tait, arXiv:0912.3259 [hep-ph].
[2] ATLAS Collaboration, ATLAS-CONF-2010-065.
[3] CMS Collaboration, arXiv:1101.1628 [hep-ex].
[4] D. S. M. Alves, E. Izaguirre and J. G. Wacker, arXiv:1008.0407 [hep-ph].
[5] H. Baer, C. Chen, F. Paige *et al.*, Phys. Rev. **D52** (1995) 2746-2759. I. Hinchliffe, F. E. Paige, M. D. Shapiro *et al.*, Phys. Rev. **D55** (1997) 5520-5540; L. Randall, D. Tucker-Smith, Phys. Rev. Lett. **101** (2008) 221803; A. J. Barr, C. Gwenlan, Phys. Rev. **D80** (2009) 074007.
[6] G. Aad *et al.* [ATLAS Collaboration], JINST **3** (2008) S08003.
[7] G. L. Bayatian *et al.* [CMS Collaboration], J. Phys. G **34** (2007) 995.
[8] for an early correct description of one jet over its entire p_T range see: M. Bengtsson and T. Sjostrand, Phys. Lett. B **185** (1987) 435; M. Bengtsson and T. Sjostrand, Nucl. Phys. B **289** (1987) 810; G. Miu and T. Sjostrand, Phys. Lett. B **449** (1999) 313; E. Norrbin and T. Sjostrand, Nucl. Phys. B **603** (2001) 297; M. H. Seymour, Nucl. Phys. **B436** (1995) 443-460; M. H. Seymour, Comput. Phys. Commun. **90** (1995) 95-101; G. Corcella, M. H. Seymour, Nucl. Phys. **B565** (2000) 227-244.
[9] S. Catani, F. Krauss, R. Kuhn *et al.*, JHEP **0111** (2001) 063; F. Krauss, JHEP **0208** (2002) 015.
[10] S. Höche, F. Krauss, S. Schumann and F. Siegert, JHEP **0905** (2009) 053.
[11] M. L. Mangano, M. Moretti and R. Pittau, Nucl. Phys. B **632** (2002) 343 .
[12] T. Gleisberg, S. Höche, F. Krauss, M. Schönherr, S. Schumann, F. Siegert and J. Winter, JHEP **0902** (2009) 007.
[13] M. L. Mangano, M. Moretti, F. Piccinini *et al.*, JHEP **0307** (2003) 001.
[14] J. Alwall, P. Demin, S. de Visscher *et al.*, JHEP **0709** (2007) 028.
[15] A. Buckley, J. Butterworth, S. Gieseke *et al.*, arXiv:1101.2599 [hep-ph].
[16] J. Alwall, S. Höche, F. Krauss *et al.*, Eur. Phys. J. **C53** (2008) 473-500.
[17] S. D. Ellis, R. Kleiss, W. J. Stirling, Phys. Lett. **B154** (1985) 435.
[18] V. M. Abazov *et al.* [D0 Collaboration], Phys. Lett. **B658** (2008) 112-119; T. Aaltonen *et al.* [CDF - Run II Collaboration], Phys. Rev. Lett. **100** (2008) 102001.
[19] ATLAS Collaboration, arXiv:1012.5382 [hep-ex].
[20] for a review see *e.g.* A. J. Barr, C. G. Lester, J. Phys. G **G37** (2010) 123001.
[21] M. Cacciari, G. P. Salam, G. Soyez, JHEP **0804** (2008) 063.
[22] M. Cacciari and G. P. Salam, Phys. Lett. B **641** (2006) 57; M. Cacciari, G. P. Salam and G. Soyez, <http://fastjet.fr>.
[23] F. A. Berends, W. T. Giele, H. Kuijf, R. Kleiss and W. J. Stirling, Phys. Lett. B **224** (1989) 237; F. A. Berends, H. Kuijf, B. Tausk *et al.*, Nucl. Phys. **B357** (1991) 32.
[24] C. F. Berger, Z. Bern, L. J. Dixon *et al.*, arXiv:1009.2338 [hep-ph].
[25] H. L. Lai, M. Guzzi, J. Huston, Z. Li, P. M. Nadolsky, J. Pumplin and C. P. Yuan, Phys. Rev. D **82** (2010) 074024.
[26] F. Krauss, A. Schälicke, S. Schumann *et al.*, Phys. Rev. **D70** (2004) 114009; V. M. Abazov *et al.* [DØ Collaboration], Phys. Lett. **B693** (2010) 522-530; S. Höche, S. Schumann, F. Siegert, Phys. Rev. **D81** (2010) 034026; G. Aad *et al.* [ATLAS Collaboration], arXiv:1012.5382 [hep-ex]; DØ Collaboration, Note 6032-CONF; F. A. Dias, E. Nurse and G. Hesketh, arXiv:1102.0917 [hep-ph]; ATLAS Collaboration, arXiv:1102.2696 [hep-ex].

- [27] ATLAS Collaboration, ATLAS-CONF-2010-084.
- [28] T. Plehn, D. Rainwater, P. Z. Skands, Phys. Lett. **B645** (2007) 217-221.
- [29] J. Alwall, S. de Visscher, F. Maltoni, JHEP **0902** (2009) 017.
- [30] T. Plehn and T. M. P. Tait, J. Phys. G **36** (2009) 075001.
- [31] M. Bahr, S. Gieseke, M. A. Gigg *et al.*, Eur. Phys. J. **C58** (2008) 639-707.
- [32] W. Beenakker, R. Höpker, M. Spira and P. M. Zerwas, Nucl. Phys. B **492** (1997) 51; T. Plehn, arXiv:hep-ph/9809319; www.thphys.uni-heidelberg.de/~tplehn/prospino
- [33] B. C. Allanach, Comput. Phys. Commun. **143** (2002) 305-331.
- [34] P. Z. Skands, B. C. Allanach, H. Baer *et al.*, JHEP **0407** (2004) 036.
- [35] M. Mühlleitner, A. Djouadi, Y. Mambrini, Comput. Phys. Commun. **168** (2005) 46-70.
- [36] T. Sjostrand, S. Mrenna, P. Z. Skands, JHEP **0605** (2006) 026.
- [37] B. C. Allanach *et al.*, Eur. Phys. J. C **25** (2002) 113.
- [38] J. Alwall, M. -P. Le, M. Lisanti, J. G. Wacker, Phys. Rev. **D79** (2009) 015005.
- [39] C. Englert, T. Plehn, P. Schichtel, and S. Schumann, in preparation.
- [40] R. Barate *et al.* [LEP Working Group for Higgs boson searches], Phys. Lett. B **565** (2003) 61.
- [41] T. Junk, Nucl. Instrum. Meth. A **434** (1999) 435, CDF Note 8128 [cdf/doc/statistics/public/8128], CDF Note 7904 [cdf/doc/statistics/public/7904].
- [42] H. Hu and J. Nielsen, in 1st Workshop on Confidence Limits, CERN 2000-005 (2000) [arXiv:physics/9906010]; K. Cranmer and T. Plehn, Eur. Phys. J. C **51** (2007) 415; A. De Rujula, J. Lykken, M. Pierini *et al.*, Phys. Rev. **D82** (2010) 013003; Y. Gao, A. V. Gritsan, Z. Guo *et al.*, Phys. Rev. **D81** (2010) 075022; D. E. Soper and M. Spannowsky, JHEP **1008** (2010) 029.
- [43] J. Neyman and E. S. Pearson, Philosophical Transactions of the Royal Society of London. Series A Vol. 231, (1933), pp. 289-337.